A Gas-Phase Study of the Preferential Solvation of Mn²⁺ in Mixed Water/Methanol Clusters

Bridgette J. Duncombe,[a,*] Jens O. S. Rydén,[b] Ljilijana Puškar,[b,†]
Hazel Cox,[b] and Anthony J. Stace[a]

[a] Department of Physical Chemistry, School of Chemistry, University of Nottingham, University Park, Nottingham, United Kingdom
[b] Department of Chemistry, University of Sussex, Brighton, United Kingdom

The kinetic shift that exists between two competing unimolecular fragmentation processes has been used to establish whether or not gas-phase Mn²⁺ exhibits preferential solvation when forming mixed clusters with water and methanol. Supported by molecular orbital calculations, these first results for a metal dication demonstrate that Mn²⁺ prefers to be solvated by methanol in the primary solvation shell.   (J Am Soc Mass Spectrom 2008, 19, 520–530) © 2008 American Society for Mass Spectrometry

Significant progress has been made in the development of gas-phase experiments designed to provide a molecular view of metal cation solvation [1, 2]. Early work concentrated on singly charged ions; however, in recognition of the fact that the charge state of most metals in solution is >+1, recent experiments have focused on the more challenging problem of generating and studying multiply charged cations in the gas phase [3]. To date, experiments in this direction have been primarily concerned with one-component solvent systems, e.g., $[Cu(H_2O)_N]^{2+}$ [4–9], but equally important is behavior in many-component solvents, where competing interactions may be dominated by differences in molecular properties [10–12]. In general, a condensed phase solution containing solvents with very similar pure-state properties might be expected to behave in a manner that reflects the composition of the solvent mixture [13]. There have been several attempts to simulate the behavior of metal dications in mixed solvent systems, [14–18], and of particular significance to the work discussed here are the molecular dynamics studies of Day and Patey [14, 15]. From simulations of an ion in the presence of water and methanol they concluded that a positively charged solute exhibits a pronounced preference for water. If there are large differences in the solvating abilities of the components, selective or preferential solvation may occur [11, 12]; however, the degree of averaging present in a typical condensed phase system means that subtle effects due to small differences in free energy are unlikely to make

their presence felt [13]. In contrast, the consequences of small, individual differences in molecular properties can be amplified in the gas phase because of the influence they may have on establishing equilibria or determining fragmentation pathways [10, 19–21]. Presented here are the results of a study designed to see if an established technique for generating multiply charged metal/solvent complexes in the gas phase can yield useful information on behavior in mixed solvent systems. From this first study, the experimental results demonstrate that for water and methanol as solvents, gas-phase Mn²⁺ does exhibit preferential solvation. This conclusion is supported by detailed molecular orbital calculations on a wide range of mixed $[Mn(MeOH)_N(H_2O)_P]^{2+}$ complexes, which show that small differences in the binding energies of methanol and water are sufficient to account for the experimental results.

Experimental

The experimental apparatus used for the generation and detection of gas-phase multiply charged metal-ligand complexes has been described extensively in previous publications [22]. Briefly, mixed neutral argon/ligand clusters are produced by the adiabatic expansion of solvent vapor mixed with argon through a pulsed supersonic nozzle. Previous work on the preferential solvation of hydrogen ions in clusters composed of methanol and water showed that the composition of ionized clusters depended quite significantly on the composition of the coexpansion mixture [19]. In this study, several mixtures were evaluated, but it was found that a ratio of 5:1, methanol:water, was most successful in producing manganese-methanol/water cluster ions with a distribution weighted towards one water molecule per complex. Neutral clusters of varying composition including Ar_M, $[Ar_M(CH_3OH)_N(H_2O)_P]$, and $[(CH_3OH)_N(H_2O)_P]$

Address reprint requests to Professor A. J. Stace, Department of Physical Chemistry, School of Chemistry, University of Nottingham, University Park, Nottingham NG7 2RD, United Kingdom. E-mail: anthony.stace@nottingham.ac.uk

* Current address: School of Chemistry, The University of Edinburgh, Joseph Black Building, The King's Buildings, West Mains Road, Edinburgh EH9 3JJ.

† Current address: School of Chemistry, Monash University, Box 23, Victoria 3800, Australia.

are produced during the expansion process, and these pass over a region where manganese vapor ($\sim 10^{-2}$ mbar) is generated by a Knudsen effusion cell (DCA Instruments, EC-40-63-21) operating at 1050 °C. Neutral manganese atoms collided with the molecular beam of clusters to produce various neutral clusters including some of the form $Mn(CH_3OH)_N(H_2O)_P$, where N and P are integers.

Neutral clusters enter the ion source of a high-resolution reverse geometry double focusing mass spectrometer (VG-ZAB-E) and are ionized by high-energy electron impact (~ 70–100 eV). The positively charged clusters are then accelerated at 5 kV through a field free region (first *ffr*) into the magnetic sector of the instrument where they are selected according to their mass to charge ratio. Before their detection, it is highly likely that extensive evaporation of ligands, predominantly argon but also methanol and water molecules, takes place, thus reducing the internal energy content of the metallic complexes to a relatively stable level. Accordingly, under most experimental conditions, no metal-containing ion complexes of the form $[M(L)_N(Ar)_M]^{z+}$ were detected. Argon atom evaporation appears to be a key feature in the dispersal of energy both from the pick-up collision with a metal atom and energy imparted on ionization. Since the beam entering the mass spectrometer consists predominantly of solvent clusters, a shutter at the exit of the oven is used to confirm the presence of manganese.

Two types of experiments were performed on the complexes: ion intensity measurements and mass analyzed ion kinetic energy spectroscopy (MIKES) [23]. The MIKES technique was employed to analyze the relative stability and chemical reactivity of ions in the series: $[Mn(CH_3OH)_N(H_2O)_{1 \text{ or } 2}]^{2+}$, where N covers the range 3, 4, 5. Unimolecular (metastable) decay pathways and those promoted through collisional activation were recorded by using the magnet to select ions of a particular *m/z*, and then scanning the electrostatic analyzer to detect processes taking place in the second field free region (second *ffr*) of the mass spectrometer. For studies of unimolecular decay, the background pressure in the flight tube was maintained at below 5×10^{-8} mbar; for collisional activation experiments, air was introduced into a collision cell in the second *ffr* via a needle valve to a point where the precursor ion intensity was reduced by $\sim 50\%$, ($\sim 10^{-6}$ mbar). For MIKES experiments on doubly-charged ions it is important to scan the electrostatic analyzer (ESA) from 10 keV to zero to collect singly-charged fragment ions that have masses greater than half that of the precursor ion. Recent experiments have shown that, for dications with a laboratory-frame kinetic energy of 5 keV, the most common charge reduction process is electron capture from the collision gas [24]. In cases where air is used as the collision gas, separate experiments have shown that oxygen and nitrogen have comparable efficiencies as electron donors [24].

Computational

The geometries and binding energies of $[Mn(H_2O)_N]^{2+}$, $[Mn(CH_3OH)_N]^{2+}$, $N = 1$–6, and $[Mn(CH_3OH)_N(H_2O)_P]^{2+}$, were $N + P = 2 - 6$ and $P \leq 2$, have been calculated using the Gaussian 03 suite of programs [25]. In all cases, only the high-spin state has been considered and various structural isomers involving both the first and second coordination shell will be presented.

Previous work from this group involving Mn^{2+} solvation focused on single component complexes of the form $[Mn(H_2O)_N]^{2+}$ and $[Mn(CH_3OH)_N]^{2+}$ complexes, $N = 1$–6 [26], and where their structures and binding energies were calculated using DFT (ADF; BP86/ TZP). The calculations showed that both $[Mn(H_2O)_4]^{2+}$ and $[Mn(CH_3OH)_4]^{2+}$ adopt stable tetrahedral configurations (the ^6S high-spin state was energetically the most favorable state), similar to those proposed for biochemical systems where solvent availability and coordination is restricted. The addition of further solvent molecules to the stable $N = 4$ unit showed a preference for $[Mn(ROH)_4(ROH)_{1 \text{ or } 2}]^{2+}$ structures, where the extra molecules occupy hydrogen-bonded sites in the form of a secondary solvation shell. These results indicated that double acceptor hydrogen bonds were influential in the development of cluster structure in the gas phase.

However, a recent review by Rotzinger [27] on the performance of molecular orbital methods and density functional theory in the computation of geometries and energies of metal aqua ions has shown that DFT has several limitations. In particular, the metal-ligand and hydrogen bond strengths are not balanced correctly, especially in complexes exhibiting a high (≥ 2) charge, and current popular functionals appear to favor lower coordination number. Thus, contrary to the DFT results referred to above, MP2 calculations found the $[Mn(H_2O)_6]^{2+}$ structure to be energetically more favorable than the $[Mn(H_2O)_4(H_2O)_2]^{2+}$ structure.

Therefore, in all of the work presented here, calculations have been performed at the MP2 level of theory. Given that high-spin Mn^{2+} has a half-filled 3d shell, static electron correlation is absent and thus MP2 is a perfectly adequate (and noncontroversial) method to model systems in which only dynamic electron correlation is prevalent. Geometry optimizations and frequency calculations were performed at the HF/6-31G(d) level to ensure that minima were achieved. Further optimizations were then performed at the MP2/6-311G(d, p) level.

Results and Discussion

For a cluster composed of a central ion and two distinguishable solvent species, use can be made of the unimolecular (metastable) fragmentation pattern of the cluster to identify which solvent the ion prefers. The phenomenon underpinning this approach to studying preferential solvation is called the compet-

itive shift, and a quantitative analysis in terms of competing rate constants has been given a number of years ago [19, 20]. Briefly, if an ion is to undergo unimolecular (metastable) decay in a mass spectrometer, it has to have a lifetime (t_A) with respect to decay that is approximately equal to the time taken ($\sim 5 \times 10^{-5}$ s) to travel from the ion source to the point of observation, which in this case is the second *ffr* between the magnetic and electric sectors of the instrument. If the ion has two accessible fragmentation pathways

$$A^+ \xrightarrow{k_1} B^+ \tag{1}$$

$$A^+ \xrightarrow{k_2} C^+ \tag{2}$$

with activation energies in the order $\varepsilon_1 < \varepsilon_2$ and is to undergo metastable decay via step (1), $1/k_1(E) \approx t_A$, where k_1 is the unimolecular rate constant for an internal energy of E. Under these circumstances, any small difference in activation (binding) energy between steps (1) and (2) will mean that $k_1(E) \gg k_2(E)$. Likewise, when $1/k_2(E^*) \approx t_A$, where $E^* > E$, $k_1(E^*)$ will still be $\gg k_2(E^*)$, and so step (2) will not be sufficiently competitive to yield a metastable reaction product. This kinetic analysis shows that the more facile of the two reaction pathways will generate a metastable reaction product, which in terms of simple bond fission means loss of the solvent molecule with the lower binding energy. Previously, this approach has been used to discuss preferential proton solvation in mixed water/alcohol [19, 20] and water/amine clusters [21], and supporting calculations on the unimolecular kinetics of the process show the competition to produce a metastable peak to be sensitive to binding energy differences of just 3 to 4 kJ mol^{-1} [20].

Precursor Ion Intensity Distribution of [Mn(CH$_3$OH)$_N$(H$_2$O)$_1$]$^{2+}$ Complexes

Previous calculations on the systems [Mn(H$_2$O)$_N$]$^{2+}$ and [Mn(CH$_3$OH)$_N$]$^{2+}$ in the gas phase provided evidence of stable primary solvation shells consisting of four ligand molecules bound directly to the central Mn^{2+} ion (high spin, d^5 configuration) [26]. Experimental confirmation of the stability of the underlying four-molecule unit came in the form of intensity distributions and the observation that larger clusters in the series [Mn(CH$_3$OH)$_N$]$^{2+}$, preferentially fragment down to [Mn(CH$_3$OH)$_4$]$^{2+}$ following collisional activation [26].

Figure 1 shows a precursor ion intensity distribution recorded for [Mn(MeOH)$_N$(H$_2$O)]$^{2+}$ complexes with N in the range 2–8. These particular experiments involved measuring ion intensity differences with the shutter over the oven either open or closed and, to minimize error, datasets were recorded several times over a number of days. The minimum size for a stable cluster with respect to charge-transfer was found to be [Mn(MeOH)$_2$(H$_2$O)]$^{2+}$, which matches earlier observa-
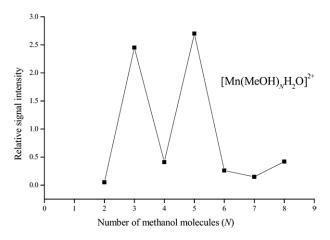

Figure 1. Precursor ion intensity distribution for complexes of the form [Mn(MeOH)$_N$H$_2$O]$^{2+}$. Note that the total number of solvent molecules surrounding the ion is $N + 1$. The data points represent averages from measurements taken at different times over a period of several days.

tions on Mn^{2+}/methanol where the minimum size was found to be [Mn(MeOH)$_3$]$^{2+}$ [26]. Of particular significance in Figure 1, are the two local maxima seen at $N = 3$ and $N = 5$, which correspond to ions with the composition [Mn(MeOH)$_3$(H$_2$O)]$^{2+}$ and [Mn(MeOH)$_5$(H$_2$O)]$^{2+}$, respectively. These results contrast with the pure solvent complexes where a single maximum at $N = 4$ was found for all of the solvents studied [26]. However, the latter did exhibit plateaux in intensity at $N \geq 5$, which has been linked to larger conformers involving structures with extended networks of hydrogen bonds [26]. For this particular mixed solvent system, it is quite possible that the profile of the intensity distribution is strongly influenced by the relative binding energies of the molecules concerned, and we shall return to a discussion of this point later. Work on singly charged mixed solvent systems by Vaden and Lisy has shown that although coordination numbers in the gas phase for systems capable of hydrogen bonding are often lower than in the condensed phase they are very dependent on ion-ligand interactions and thus, by varying the ratio of solvents, direct coordination to the central metal ion can be modified [11, 12].

MIKE Spectra: Unimolecular and Collision-Induced Dissociation Studies of [Mn(CH$_3$OH)$_N$(H$_2$O)]$^{2+}$ Complexes

To utilize the competitive shift as a mechanism for probing relative binding energy, experiments have been undertaken using the MIKES technique to detect both metastable decay and the effects of collisional activation. Three ions of mixed composition are considered in this first section, and these are: [Mn(MeOH)$_3$(H$_2$O)]$^{2+}$, [Mn(MeOH)$_4$(H$_2$O)]$^{2+}$, and [Mn(MeOH)$_5$(H$_2$O)]$^{2+}$. For each of the complexes, the single water molecule acts as a probe of relative binding energy with the metal dication. If the water molecule falls off, it is obviously the more weakly bound of the two solvents—an effect
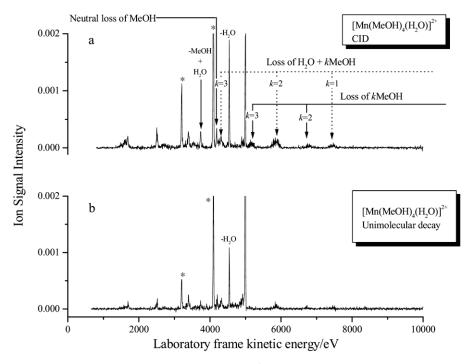
Figure 2. MIKE scan recorded for $[Mn(MeOH)_4H_2O]^{2+}$ under separate conditions where collision-induced dissociation (CID) and unimolecular decay should prevail.

that even overrides any statistical contribution from an increasing number of methanol molecules [19]. For the series of ions under consideration, two neutral loss processes are most likely to be in competition and these are:

$$[Mn(MeOH)_N(H_2O)]^{2+} \rightarrow [Mn(MeOH)_{N-1}(H_2O)]^{2+}$$
$$+ MeOH \qquad (3)$$

$$[Mn(MeOH)_N(H_2O)]^{2+} \rightarrow [Mn(MeOH)_N]^{2+} + H_2O \quad (4)$$

Figure 2 shows examples of two MIKE scans recorded on the ion $[Mn(MeOH)_4(H_2O)]^{2+}$: Figure 2a shows the result of collisional activation and Figure 2b is the unimolecular signal. Although the ion signals are weak and susceptible to interference from underlying ions, the resolution is sufficient to allow identification of

fragments arising from both neutral loss and charge reduction processes. Fortunately, none of the interfering peaks (some denoted with *) have masses that coincide with those of any fragment ions that could sensibly originate from the precursor ions. Table 1 summarizes the most important fragmentation pathways observed for ions with N = 3, 4, and 5. The dominant unimolecular loss is that of the single neutral water molecule and even the introduction of a collisional gas does not induce other significant neutral loss channels. Despite the statistical advantage of there being more methanol molecules in all of the complexes, loss of that molecule in isolation does not feature prominently. When it does occur, methanol loss is frequently accompanied by the simultaneous loss of water; suggesting either a sequential reaction or the loss of the two molecules as a single unit (see below).

Table 1. Summary of the fragmentation pathways observed following the unimolecular and collision-induced dissociation (CID) of $[Mn(MeOH)_N(H_2O)_P]^{2+}$ cluster ions for N = 3, 4, and 5, and P = 1 and 2

Ion	Dominant unimolecular pathway	CID pathways (neutral loss)	CID pathways (charge reduction)
$[Mn(MeOH)_3(H_2O)]^{2+}$	H_2O	$H_2O > CH_3OH.$	$(H_2O + kCH_3OH; k = 1,2), (kCH_3OH; k = 1,2).$
$[Mn(MeOH)_4(H_2O)]^{2+}$	H_2O	$H_2O > (CH_3OH + H_2O) > CH_3OH.$	$(H_2O + kCH_3OH; k = 1–3), (kCH_3OH; k = 2,3).$
$[Mn(MeOH)_5(H_2O)]^{2+}$	H_2O	$H_2O > (CH_3OH + H_2O) > CH_3OH.$	$(H_2O + kCH_3OH; k = 2–4).$
$[Mn(MeOH)_3(H_2O)_2]^{2+}$	H_2O	$H_2O > CH_3OH + 2H_2O.$	$(H_2O + kCH_3OH; k = 1,2), (2H_2O + kCH_3OH; k = 1,2).$
$[Mn(MeOH)_4(H_2O)_2]^{2}$	H_2O	$H_2O > 2H_2O > (CH_3OH + H_2O) > (CH_3OH + 2H_2O) > CH_3OH.$	$(H_2O + kCH_3OH; k = 2,3), (2H_2O + kCH_3OH; k = 1,2)$

The dominant electrostatic contributions to bonding within the clusters are ion-dipole and ion-induced dipole interactions, as defined by

$$V(r) \propto -\frac{\alpha z^2}{r^4} - \frac{z\mu}{r^2} \quad (5)$$

where z is the charge on the ion, r is the ion-molecule distance, α is the polarizability, and μ is the dipole moment. Since the dipole term varies as $1/r^2$, this will have an effect on binding over a longer range than the polarizability term, which varies as $1/r^4$. However, the latter is proportional to the square of the charge and so could become significant at short range. This is particularly relevant in this case as the dipole moment of water (1.85 D) is only slightly larger than that of methanol (1.70 D). Calculations involving eq 5 show that the higher polarizability of methanol (3.23 Å^3) with respect to water (1.48 Å^3) has the dominant influence on bonding, and that at distances <8 Å, eq 5 predicts that methanol should always be more strongly bound than water to the dication. This result provides semiquantitative support for the experimental observations.

Collisional activation studies are of interest because this process imparts additional energy to the precursor ion and so the lifetime constraint discussed above no longer applies. As a result, higher internal energies are involved leading to a greater variety of dissociation processes which, for smaller multiply charged ions, include charge separation and electron capture. The singly charged products of these reactions are frequently observed above 5000 eV on the energy scale in a MIKE scan, which is fortuitous as this region is completely unaffected by any underlying coincidental singly charged ions and as such aids identification of the precursor ion and associated dissociation pathways. Based on recent evidence from other experiments [24, 28], it is highly probable that, following collisional activation, each of the ions studied exhibits charge reduction followed by a variety of fragmentation pathways. The broad weak features (see for example Figure 2a) associated with these pathways do not have sufficient intensity for individual reaction steps to be resolved; however, the peaks are centered on fragment ion masses equivalent to combinations of the following reactions:

$$[\text{Mn(MeOH)}_N\text{H}_2\text{O}]^{2+} \rightarrow [\text{MeOMn(MeOH)}_{N-K-1}$$
$$(\text{H}_2\text{O})]^+ + K\text{MeOH} + \text{H} \quad (6a)$$

$$\rightarrow [\text{Mn(MeOH)}_{N-K}(\text{H}_2\text{O})]^+$$
$$+ K\text{MeOH} \quad (6b)$$

$$\rightarrow [\text{MeOMn(MeOH)}_{N-K-1}]^+$$
$$+ \text{H}_2\text{O} + K\text{MeOH} + \text{H} \quad (7a)$$

$$\rightarrow [\text{Mn(MeOH)}_{N-K}]^+ + \text{H}_2\text{O}$$
$$+ K\text{MeOH} \quad (7b)$$

The relative contributions from, for example, eq 6a and b have been found to be sensitive to both the nature of the collision gas and the size of the dication complex [24, 28]. There are a number of interesting features to the results, which are summarized in Table 1. First, collisional activation clearly enhances the loss of neutral water, but as the clusters increase in size, a variety of neutral fragmentation processes gain prominence including the loss of water plus one or more methanol molecules. Second, $[\text{Mn(MeOH)}_3(\text{H}_2\text{O})]^{2+}$ and $[\text{Mn(MeOH)}_4(\text{H}_2\text{O})]^{2+}$ each exhibit both of the above reactions, which contrasts with $[\text{Mn(MeOH)}_5(\text{H}_2\text{O})]^{2+}$, which only displays reaction 7. Since electron capture is very rapid in comparison to fragmentation, the underlying metal cation responsible for the broad peaks at energies >5000 eV will be singly charged. However, that cation will be created in the presence of a solvent configuration that reflects the preferences of the precursor dication. Assuming the solvent molecules do not undergo extensive rearrangement before fragmentation, the distribution of reaction products should mirror the composition (but not necessarily the binding energy) that existed for Mn^{2+}. That being the case, the continued loss of water and water + methanol serves to confirm that the site occupied by water is comparatively less stable than that occupied by any of the methanol molecules.

A consequence of the electron capture process having a comparatively large collision cross-section [29] is that low intensity charge reduction peaks are frequently seen at the very low flight tube pressures used to study unimolecular decay. Evidence of this is seen in Figure 2b where residual electron capture peaks are present at laboratory-frame kinetic energies >5000 eV. Fortunately, electron capture does not interfere with any of the neutral unimolecular processes discussed above.

Unimolecular and Collision-Induced Dissociation of $[\text{Mn(CH}_3\text{OH)}_N(\text{H}_2\text{O})_2]^{2+}$ Complexes

A limited study involving complexes of the form $[\text{Mn(MeOH)}_N(\text{H}_2\text{O})_2]^{2+}$ for $N = 3$ and 4 has also been possible under the experimental conditions outlined above. Figure 3 shows the unimolecular decay and collision induced dissociation patterns recorded for $[\text{Mn(MeOH)}_4(\text{H}_2\text{O})_2]^{2+}$, and relevant data on both complexes are given in Table 1. For each size of complex, the unimolecular loss of neutral water was again found to be the dominant decay channel. However, it is worth noting that for $[\text{Mn(MeOH)}_4(\text{H}_2\text{O})_2]^{2+}$, a comparatively intense peak corresponding to the loss of two neutral water molecules was also observed. The fragmentation channels seen in Figure 3 that are promoted by collisional activation are similar to those found for the system $[\text{Mn(MeOH)}_N(\text{H}_2\text{O})]^{2+}$, with the only significant difference being that $[\text{Mn(MeOH)}_4(\text{H}_2\text{O})_2]^{2+}$ does show more extensive loss of water accompanied by methanol, both in neutral form and as a charge reduction product.
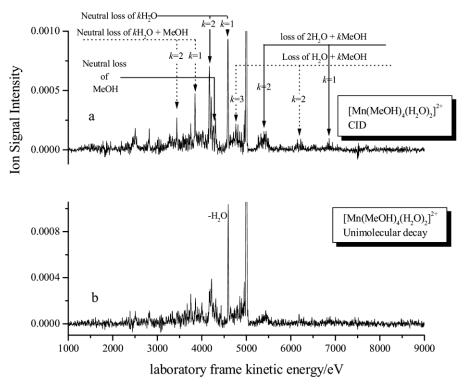
Figure 3. MIKE scan recorded for $[Mn(MeOH)_4(H_2O)_2]^{2+}$ under separate conditions where collision-induced dissociation (CID) and unimolecular decay should prevail.

Theoretical Results and Discussion

Calculated Mn(II)-Water and Mn(II)-Methanol Structures

Geometries of the $[Mn(H_2O)_N]^{2+}$ and $[Mn(CH_3OH)_N]^{2+}$ complexes for $N = 1$ to 6 were optimized using MP2/6-311G(d,p) as set out in the computational details. In addition to the most stable geometries in which all ligands were in the first coordination shell (i.e., tetrahedral for $N = 4$, square-based pyramid for $N = 5$, and octahedral for $N = 6$), structures involving up to two ligands in the second coordination shell, bonded via double acceptor hydrogen bonds to ligands in the first shell, were also considered. The notation "$X + Y$" is used to denote X ligands in the first shell and Y ligands in a second shell; for example, an octahedral complex will be denoted "6 + 0" whereas a complex with four primary shell ligands and two secondary shell ligands is denoted "4 + 2". Tables 2 and 3 give the average binding energy, which is defined as the energy required to perform the step: $[ML_N]^{2+} \rightarrow M^{2+} + NL$, and the incremental binding energy, which is defined as the energy required to perform the step: $[ML_N]^{2+} \rightarrow [ML_{N-1}]^{2+} + L$ for the Mn(II)-water and Mn(II)-methanol complexes, respectively. In all cases, the average binding energies (and hence total energies, not shown) of the Mn(II)-methanol complexes are greater than their Mn(II)-water counterparts. Surprisingly however, the difference in

Table 2. The average binding energies and incremental binding energies of $[Mn(H_2O)_N]^{2+}$ complexes calculated at the MP2/6-311G(d,p) level of theory and where N ranges from 1–6. $X + Y$ is used to denote X molecules in the primary solvation shell and Y molecules in a secondary shell. Data are given for the most stable structural isomer at each value of N

$X + Y$	Complex	Average binding energy/kJ mol^{-1}	Isomer energy difference/kJ mol^{-1}	Incremental binding energy/kJ mol^{-1}
1 + 0	$[Mn(H_2O)]^{2+}$	325.0		
2 + 0	$[Mn(H_2O)_2]^{2+}$	622.7		297.7
3 + 0	$[Mn(H_2O)_3]^{2+}$	850.70		228.0
4 + 0	$[Mn(H_2O)_4]^{2+}$	1045.3	0	194.6
3 + 1	$[Mn(H_2O)_3(H_2O)]^{2+}$	992.15	53.2	141.4
5 + 0	$[Mn(H_2O)_5]^{2+}$	1199.8	0	154.5
4 + 1	$[Mn(H_2O)_4(H_2O)]^{2+}$	1175.3	24.5	130.0
6 + 0	$[Mn(H_2O)_6]^{2+}$	1340.2	0	140.3
trans 4 + 2	$[Mn(H_2O)_4(H_2O)_2]^{2+}$	1302.0	38.1	102.2
cis 4 + 2	$[Mn(H_2O)_4(H_2O)_2]^{2+}$	1292.4	47.7	92.6

Table 3. The average binding energies and incremental binding energies of $[Mn(CH_3OH)_N]^{2+}$ complexes calculated at the MP2/6-311G(d,p) level of theory and where N ranges from 1–6. $X + Y$ is used to denote X molecules in the primary solvation shell and Y molecules in a secondary shell. Data are given for the most stable structural isomer at each value of N

$X + Y$	Complex	Average binding energy/kJ mol^{-1}	Isomer energy difference/kJ mol^{-1}	Incremental binding energy/kJ mol^{-1}
1 + 0	$[Mn(MeOH)]^{2+}$	363.1		
2 + 0	$[Mn(MeOH)_2]^{2+}$	685.9		322.8
3 + 0	$[Mn(MeOH)_3]^{2+}$	918.9		233.0
4 + 0	$[Mn(MeOH)_4]^{2+}$	1114.3	0	195.4
3 + 1	$[Mn(MeOH)_3(MeOH)]^{2+}$	1057.4	56.9	138.5
5 + 0	$[Mn(MeOH)_5]^{2+}$	1263.2	0	148.8
4 + 1	$[Mn(MeOH)_4(MeOH)]^{2+}$	1241.1	22.1	126.8
6 + 0	$[Mn(MeOH)_6]^{2+}$	1397.8	0	134.7
$trans4 + 2$	$[Mn(MeOH)_4(MeOH)_2]^{2+}$	1365.5	32.3	102.4

average binding energy between Mn(II)-methanol and Mn(II)-water for $N = 2$–6 remains fairly constant at ~64 kJ mol^{-1}. Furthermore, although the Mn(II)-water complexes are generically less stable, the energy gained on adding the Nth ligand for $N > 2$, be it water or methanol molecule, is approximately the same (the difference ranging from 0 to 6 kJ mol^{-1}).

As noted earlier, there has been some comment on the validity of using DFT to model metal-aqua ions, as the theory appears to overestimate hydrogen-bonding and favor lower coordination when compared with wave function-based methods such as MP2. The data in Tables 2 and 3 clearly show that, in all cases, the higher coordination "$N + 0$" structures are favored over the hydrogen bonded structures. The relative energy differences between isomers are also given in Tables 2 and 3, for water and methanol complexes, respectively. For the $N = 4$ structures, the primary shell tetrahedral geometry is clearly favored (as it is with DFT). However, for geometries when $N = 5$ and 6, MP2 favours the "$N + 0$" structures, which is quite different from the DFT results. However, the energy difference between the "5 + 0" and "4 + 1" complexes is less than 25 kJ mol^{-1}, regardless of ligand, which means that both isomers could be accessible during an experiment of the type performed here. For the $N = 6$ water complexes, the energy difference between the octahedral and trans-hydrogen bonded isomers is slightly higher at 38 kJ mol^{-1};

when the two second-shell water molecules are placed in the cis geometry, increased ligand–ligand repulsion destabilizes that complex by a further 10 kJ mol^{-1}. The cis structure is not possible for the methanol complex given that double acceptor hydrogen bonds are formed. If a cis $N = 6$ methanol configuration composed of single hydrogen bonds is adopted as a starting structure, it rapidly resorts to one double and one single acceptor hydrogen bond which, in turn, is less stable than the trans configuration discussed above. The energy difference between the octahedral "6 + 0" and the hydrogen-bonded "4 + 2" Mn(II)-methanol complexes is about 32 kJ mol^{-1}.

As expected, the incremental binding energy declines as the number of ligands increases due to the competition for the positive charge. However, when only the most stable "$N + 0$" structures are considered, the plateau at $N = 4$ is indicative of preferential stability. Interestingly, the energy gained on adding a fourth ligand to either $[Mn(H_2O)_3]^{2+}$ or $[Mn(CH_3OH)_3]^{2+}$ is essentially the same for both complexes (194.6 kJ mol^{-1} compared with 195.4 kJ mol^{-1}, respectively).

Calculated Mixed-Ligand Structures

Geometries of the mixed ligand complexes $[Mn(CH_3OH)_N(H_2O)_P]^{2+}$, where $P = 1$ or 2 and $N + P = 2$ to 6, were optimized using MP2/6-311G(d,p) and their energetics are presented in Table 4 for $P = 1$ and

Table 4. The average binding energies and incremental binding energies of $[Mn(CH_3OH)_N(H_2O)]^{2+}$ complexes calculated at the MP2/6-311G(d,p) level of theory and where N ranges from 1–5. $X + Y$ denotes X ligands in the first coordination shell and Y ligands in the second. The incremental binding energies for methanol (MeOH) were calculated according to eq 8 and for water (H$_2$O) according to eq 9. Data are given for the most stable structural isomers at each value of $N + 1$

$X + Y$	Complex	Av. binding energy/kJmol^{-1}	Incremental binding energy (MeOH)/kJmol^{-1}	Incremental binding energy (H$_2$O)/kJmol^{-1}
2 + 0	$[Mn(MeOH)(H_2O)]^{2+}$	655.2		292.1
3 + 0	$[Mn(MeOH)_2(H_2O)]^{2+}$	897.4	242.2	211.5
4 + 0	$[Mn(MeOH)_3(H_2O)]^{2+}$	1097.2	199.8	178.3
3 + 1	$[Mn(MeOH)_3(H_2O)]^{2+}$	1046.1		
5 + 0	$[Mn(MeOH)_4(H_2O)]^{2+}$	1251.1	153.8	136.7
4 + 1	$[Mn(MeOH)_4(H_2O)]^{2+}$	1231.1		
6 + 0	$[Mn(MeOH)_5(H_2O)]^{2+}$	1388.8	137.8	125.7
5 + 1	$[Mn(MeOH)_5(H_2O)]^{2+}$	1361.8		
4 + 2	$[Mn(MeOH)_5(H_2O)]^{2+}$	1357.8		

Table 5. The average binding energies and incremental binding energies of $[Mn(CH_3OH)_N(H_2O)_2]^{2+}$ complexes calculated at the MP2/6-311G(d,p) level of theory and where N ranges from 1–4. $X + Y$ denotes X ligands in the first coordination shell and Y ligands in the second. The incremental binding energies for methanol (MeOH) were calculated according to eq 8 and for water (H_2O) according to eq 9. ($2\times H_2O$) denotes the loss of both waters with the value in brackets being the energy per water. Data are given for the most stable structural isomer at each value of $N + 2$

$X + Y$	Complex	Av. binding energy/kJ mol^{-1}	Incremental binding energy (H_2O)/kJ mol^{-1}	Incremental binding energy (MeOH)/kJ mol^{-1}	Incremental binding energy ($2\times H_2O$)/kJ mol^{-1}
4 + 0	$[Mn(MeOH)_2(H_2O)_2]^{2+}$	1080.4	182.9		394.4 (197.2)
5 + 0	$[Mn(MeOH)_3(H_2O)_2]^{2+}$	1239.5	142.4	159.2	320.6 (160.3)
4 + 1	$[Mn(MeOH)_3(H_2O)_2]^{2+}$	1216.8			
3 + 2	$[Mn(MeOH)_3(H_2O)_2]^{2+}$	1216.8			
6 + 0	$[Mn(MeOH)_4(H_2O)_2]^{2+}$	1379.0	128.0	139.5	264.7 (132.4)
5 + 1	$[Mn(MeOH)_4(H_2O)_2]^{2+}$	1350.5			
4 + 2	$[Mn(MeOH)_4(H_2O)_2]^{2+}$	1347.2			

Table 5 for $P = 2$. For comparison, complexes of the form $[Mn(H_2O)_N(CH_3OH)_P]^{2+}$, where the water molecules remain in the inner shell, and where $P = 1$ or 2 and $N + P = 5$ or 6, were also optimized, and these data are presented in Table 6. Structures that involved both the primary solvation shell as well as those with up to two ligands in a second shell were considered in all cases. Again, the notation "$X + Y$" will be used to denote X ligands in the first shell and Y ligands in a second shell. For example, "6 + 0" $[Mn(CH_3OH)_4(H_2O)_2]^{2+}$ refers to a mixed-ligand octahedral structure, whereas "4 + 2" refers to a primary shell of four methanol molecules with two water molecules forming a second solvation shell coordinated to the first via hydrogen bonding.

Tables 4, 5, and 6 give average binding energies which are defined as the energy required to perform the step: $[ML1_NL2_P]^{2+} \rightarrow M^{2+} + NL1 + PL2$, and incremental binding energies, which are generally defined as the energy required to perform the step: $[ML1_NL2_P]^{2+} \rightarrow [ML1_NL2_{P-1}]^{2+} + L2$, where L1 and L2 represent either methanol or water molecules. In all cases, the formation of a primary solvation shell is preferable over the promotion of one or two ligands to a second solvation shell. The relative energy differences between the various structural isomers have reduced slightly; for $N = 4$, 5, and 6 the isomer differences are 51, 20, and 27 kJ mol^{-1}, respectively, for the Mn(II)-methanol-one-water complexes compared with 57, 22, 32 kJ mol^{-1}, respectively, for the Mn(II)-methanol only complexes. The

isomer energy differences are again quite similar for the methanol with two water complexes, i.e., 23 and 28 kJ mol^{-1} for $N = 5$ and 6, respectively. Following the trends discussed in the previous section, complexes that are predominantly methanol are more stable than their analogous water counterparts.

The replacement of a methanol molecule with water serves to destabilize a Mn(II)-methanol complex and conversely the addition of a methanol molecule to a Mn(II)-water complex results in an increase in average binding energy. However, these changes are relatively small (replacing a methanol molecule with water in the "4 + 0" methanol structure decreases the binding energy by 17 kJ mol^{-1}, by 12 kJ mol^{-1} in the "5 + 0", and by 9 kJ mol^{-1} in the "6 + 0"). The trend seems consistent as replacing a second methanol to form the "6 + 0" $[Mn(CH_3OH)_4(H_2O)_2]^{2+}$ complex costs another ~9 kJ mol^{-1}. Interestingly, it is only slightly more efficient (cheaper) to replace methanol molecules that were formerly in the second shell rather than in the first (i.e., "5 + 1" or "4 + 2" structures rather than "6 + 0") with water. The energy difference between the all methanol "4 + 2" structure and the "4 + 2" structure with two second shell water ligands is 18.3 kJ mol^{-1} compared with 18.8 kJ mol^{-1} in the "6 + 0" example given above. For comparison, when one or two water molecules in the Mn-water complexes were replaced with methanol, the "6 + 0"-$[Mn(H_2O)_4(CH_3OH)_2]^{2+}$ is more stable than the "6 + 0"-$[Mn(H_2O)_6]^{2+}$ by 17.6 kJ mol^{-1}. However, the gain in energy due to replacement

Table 6. The average binding energies and incremental binding energies of $[Mn(H_2O)_N(CH_3OH)_P]^{2+}$ complexes calculated at the MP2/6-311G(d,p) level of theory and where N ranges from 1–5 (or 4) and P has the values 1 or 2. $X + Y$ denotes X ligands in the first coordination shell and Y ligands in the second. The incremental binding energies for methanol (MeOH) were calculated according to eq 8 and for water (H_2O) according to eq 9

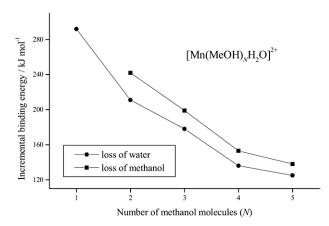| $X + Y$	Complex	Av. binding energy/kJ mol^{-1}	Relative energy difference/kJ mol^{-1}	Incremental binding energy (MeOH)/kJ mol^{-1}	Incremental binding energy (H_2O)/kJ mol^{-1}
5 + 0	$[Mn(H_2O)_4(MeOH)]^{2+}$	1212.9	0	167.6	
4 + 1	$[Mn(H_2O)_4(MeOH)]^{2+}$	1186.8	26.1		
6 + 0	$[Mn(H_2O)_5(MeOH)]^{2+}$	1350.4	0	150.5	137.5
5 + 1	$[Mn(H_2O)_5(MeOH)]^{2+}$	1331.2	19.2		
6 + 0	$[Mn(H_2O)_4(MeOH)_2]^{2+}$	1357.8	0		
4 + 2	$[Mn(H_2O)_4(MeOH)_2]^{2+}$	1322.9	35.0		

Figure 4. Plot of the incremental binding energies of water and methanol as a function of the number of methanol molecules in complexes of the form $[Mn(MeOH)_N H_2O]^{2+}$.

of second shell water molecules in the "4 + 2" structure is slightly greater (at 20.9 kJ mol^{-1}) than that of replacing first shell waters in the "6 + 0" structure.

The incremental binding energies given in Table 4 for the mixed complexes $[Mn(MeOH)_N(H_2O)]^{2+}$ are equivalent to the activation energies necessary to promote reactions (eqs) 3 and 4 and involve the loss of either MeOH or H$_2$O. Clearly for all values of N the binding energy (and therefore the activation energy) is greater for MeOH added to $[Mn(MeOH)_{N-1}(H_2O)]^{2+}$ than when a H$_2$O is added to $[Mn(MeOH)_N]^{2+}$. This trend equates well with the observed prominent unimolecular loss of a single neutral water molecule. The energy difference ranges from ~30 kJ mol^{-1} at $N = 2$ to just 12 kJ mol^{-1} at $N = 5$, which from earlier calculations lies above the energy threshold identified as necessary for the competitive shift to operate effectively [20].

Figure 4 shows incremental binding energies for reaction steps [3] and [4]. It can be seen that at $N + P = 4$ (3 methanol and 1 water) there is a plateau of stability. This would imply preferential stability for this coordination number and agrees well with the intensity distribution shown in Figure 2. However, it is interestingly to note that this plateau is less pronounced for the addition (or loss) of a MeOH molecule than when compared with the addition (or loss) of a water molecule (second difference is 33 kJ mol^{-1} versus 42 kJ mol^{-1} when adding a fourth water and methanol, respectively, compared with 42 and 46 kJ mol^{-1} when adding the fifth water and methanol, respectively). Thus, given the data in Figure 2 and Table 1, this may be further evidence that water loss is preferable.

Table 5 shows data calculated for mixed complexes containing two water molecules, where again it can be seen that H$_2$O loss is preferred to MeOH loss as the energy gained on adding a methanol (eq 8) is greater than the energy gained on adding a water molecule (eq 9).

$$[Mn(MeOH)_N(H_2O)_2]^{2+} \rightarrow [Mn(MeOH)_{N-1}(H_2O)_2]^{2+}$$
$$+ \, MeOH \qquad (8)$$

$$[Mn(MeOH)_N(H_2O)_2]^{2+} \rightarrow [Mn(MeOH)_N(H_2O)]^{2+}$$
$$+ \, H_2O \qquad (9)$$

Furthermore, the energy required for the process is about the same as that for the mixed ligand one water complexes (within 5 kJ mol^{-1}).

Since the experiment shows that collisional activation promotes the loss of more than one molecule, it is also of interest to calculate the energy required for processes such as:

$$[Mn(MeOH)_N(H_2O)_2]^{2+} \rightarrow [Mn(MeOH)_N]^{2+} + 2H_2O$$
$$(10)$$

and these data are also shown in Table 5. Although this process takes considerably more energy, it can be seen that, per water molecule, the internal energy (shown in brackets) required by a complex to promote such reactions is competitive with steps involving the loss of methanol. In all cases (quite apart from considerations of microscopic reversibility), it is most probable that any loss of more than one molecule occurs as a sequential step. At a more subtle level, it is possible to show from the data that in the case, for example, of $[Mn(MeOH)_4(H_2O)_2]^{2+}$ it requires marginally less energy (~6 kJ mol^{-1}) to lose methanol followed by water than it does for the reverse sequence.

Finally, Table 6 presents data on mixed complexes where the dominant species is water. As can be seen, the results are consistent with the previous data in that direct coordination to the metal cation produces the most stable structures, and water molecules have lower binding energies than those of methanol. What is interesting, and this appears to be a general feature across the range of mixed clusters, is that if the calculated binding energies of the individual molecules are compared with those for the same molecule in the pure complex, it can be seen that in the mixed complexes methanol is more strongly bound and the binding energy of water declines. For example, comparing $[Mn(H_2O)_5(MeOH)]^{2+}$ in Table 6 with both single-molecule $N = 6$ complexes, i.e., Tables 2 and 3, for the mixed complex the binding energy of methanol has increased by ~16 kJ mol^{-1} and the binding energy of water has declined by ~-3 kJ mol^{-1}.

Bond Length Comparisons

As discussed above, the most stable configurations are generated when all of the ligands are directly coordinated to the central dication. Differences between methanol and water are further reflected in the calculated bond lengths as tabulated in Table 7. The average Mn(II)-methanol bond length is consistently shorter than the average Mn(II)-water bond length, but the difference decreases from about 4 pm in the $N = 1$ complex to just 0.3 pm in the octahedral complexes. However, it is interesting to note a small but significant

Table 7. Calculated bond lengths (Å) in primary solvation shell complexes of the form $[Mn(MeOH)_N(H_2O)_P]^{2+}$, where $P = 0$, 1, or 2 for the single solvent, one water and two water complexes, respectively. Results for $P = 2$ are given in brackets

	$[Mn(H_2O)_N]^{2+}$	$[Mn(MeOH)_N]^{2+}$	$[Mn(MeOH)_N(H_2O)_P]^{2+}$	
$N + P$	Mn – OH_2/Å	Mn – OH(Me)/Å	Mn – OH_2/Å	Mn-OH(Me)/Å
1 + 0	2.008	1.971		
2 + 0	2.016	1.985	2.020	1.981
3 + 0	2.067	2.044	2.092	2.034
4 + 0	2.107	2.094	2.129 (2.122)	2.086 (2.079)
5 + 0	2.161	2.149	2.165 (2.163)	2.150 (2.147)
6 + 0	2.202	2.199	2.232 (2.226)	2.194 (2.189)

change, when one or more ligands are replaced by the competitor. The Mn(II)-methanol bonds shorten and Mn(II)-water lengthen relative to their respective length in the single solvent complexes. For example, in the "$N + P = 6$"-$[Mn(CH_3OH)_4(H_2O)_2]^{2+}$ complex the water is pushed out by the methanol. This results in a 1 to 2 pm shortening of the Mn(II)-methanol bonds compared with those in the $[Mn(CH_3OH)_6]^{2+}$ complex, and a lengthening by about the same amount of the Mn(II)-water bonds. This pattern mimics that seen for the binding energies.

Conclusions

Experiments and calculations have been undertaken to study the behavior of the mixed-solvent systems $[Mn(MeOH)_N(H_2O)_{1 \text{ or } 2}]^{2+}$ in the gas phase. From all of the observed unimolecular decay processes it is concluded the water molecules are more weakly bound than any of the methanol molecules, and binding energies calculated for a wide range of both pure and mixed solvent complex support that conclusion. Likewise, decay processes promoted by collisional activation most frequently involve water, but are often accompanied by methanol in the form of a charge-transfer product.

As noted by Kebarle et al. [10], this picture of preferential solvation in the gas phase may not necessarily extend to behavior in solution. Overall stability of a fully solvated metal ion may depend on the formation of an extended network of hydrogen bonds [29], and that is more easily achieved when water (up to 8 H-bonds) rather than methanol (up to 4 H-bonds) forms a four-coordinate primary solvation shell. However, much also depends on how effective structures are at using charged enhanced hydrogen bonds to lock molecules into configurations that provide more limited access to the primary shell. Such structures may then use water molecules to develop a more extensive hydrogen bond network in subsequent shells.

A final comment should be made regarding the unexpected shape exhibited by distribution of relative ion intensities shown in Figure 1. It is highly likely that the profile is strongly influenced by a combination of preferential fragmentation and the composition of the solvent mixture at the point of expansion. Both the results presented here and those recorded previously for Mn^{2+} complexes [26] have demonstrated that complexes with four ligands are usually the most intense in any distribution. For all of the complexes associated with Figure 1, the route to their appearance as stable ions is probably via precursors that have an excess of water molecules since, of the two molecules, they are always the most weakly bound. Therefore, each $[Mn(CH_3OH)_N H_2O]^{2+}$ combination is likely to be the product of a unique fragmentation pathway, which is different from pure clusters where sequential decay would be expected. The latter process naturally favours smaller complexes, hence the relatively high intensity of the $[Mn(L)_4]^{2+}$ ion.

Acknowledgments

References

1. Kebarle, P. Ion Thermochemistry and Solvation from Gas-Phase Ion Equilibria. *Annu. Rev. Phys. Chem.* **1977,** *28,* 445–476.
2. Keesee, R. G.; Castleman, A. W., Jr. Thermochemical Data on Gas-Phase Ion-Molecule Association and Clustering Reactions. *J. Phys. Chem. Ref. Data* **1986,** *15,* 1011–1071.
3. Stace, A. J. Metal Ion Solvation in the Gas Phase: The Quest for Higher Oxidation States. *J. Phys. Chem. A* **2002,** *106,* 7993–8005.
4. Blades, A. T.; Jayaweera, P.; Ikonomou, M. G.; Kebarle, P. Ion-Molecule Clusters Involving Doubly Charged Metal Ions M^{2+}. *Int. J. Mass Spectrom. Ion Processes* **1990,** *102,* 251–267.
5. Blades, A. T.; Jayaweera, P.; Ikonomou, M. G.; Kebarle, P. Studies of Alkaline-Earth and Transition-Metal M^{2+} Gas-Phase Ion Chemistry. *J. Chem. Phys.* **1990,** *92,* 5900–5906.
6. Stace, A. J.; Walker, N. R.; Firth, S. $[Cu(H_2O)_n]^{2+}$ Clusters: The First Evidence of Aqueous Cu(II) in the Gas Phase. *J. Am. Chem. Soc.* **1997,** *119,* 10239–10240.
7. Rodrigeuz-Cruz, S. E.; Jockusch, R. A.; Williams, E. R. Hydration Energies of Divalent Metal ions, $Ca^{2+}(H_2O)_n$ (n = 5–7) and $Ni^{2+}(H_2O)_n$ (n = 6–8), Obtained by Blackbody Infrared Radiative Dissociation. *J. Am. Chem. Soc.* **1998,** *120,* 5842–5843.
8. Rodrigeuz-Cruz, S. E.; Jockusch, R. A.; Williams, E. R. Hydration Energies and Structures of Alkaline Earth Metal Ions, $M^{2+}(H_2O)_n$, n = 5–7, M = Mg, Ca, Sr, and Ba. *J. Am. Chem. Soc.* **1999,** *121,* 8898–8906.
9. Wright, R. R.; Walker, N. R.; Firth, S.; Stace, A. J. The Coordination and Chemistry of Stable Cu(II) Complexes in the Gas Phase. *J. Phys. Chem. A* **2001,** *105,* 54–64.
10. Nielsen, S. B.; Masella, M.; Kebarle, P. Competitive Gas-Phase Solvation of Alkali Metal Ions by Water and Methanol. *J. Phys. Chem. A* **1999,** *103,* 9891–9898.
11. Vaden, T. D.; Lisy, J. M. Investigation of Competing Interactions in Alkali Metal Ion-Acetone-Water Clusters. *Chem. Phys. Lett.* **2005,** *408,* 54–58.

12. Vaden, T. D.; Lisy, J. M. Competing Noncovalent Interactions in Alkali Metal Ion-Acetonitrile-Water Clusters. *J. Phys. Chem. A* **2005,** *109,* 3880–3886.
13. Marcus, Y. *Introduction to Liquid State Chemistry;* Wiley: London, 1977; p. 164.
14. Day, T. J. F.; Patey, G. N. Ion Solvation Dynamics in Binary Mixtures. *J. Chem. Phys.* **1997,** *106,* 2782–2791.
15. Day, T. J. F.; Patey, G. N. Ion Solvation Dynamics in Water-Methanol and Water Dimethylsulfoxide Mixtures. *J. Chem. Phys.* **1999,** *110,* 10937–10944.
16. Pranowo, H. D.; Rode, B. M. Simulation of Preferential Cu^{2+} Solvation in Aqueous Ammonia Solution by Means of Monte Carlo Method Including Three-Body Correction Terms. *J. Chem. Phys.* **2000,** *112,* 4212–4215.
17. Pranowo, H. D. Monte Carlo Simulation of $CuCl_2$ in 18.6% Aqueous Ammonia Solution. *Chem. Phys.* **2003,** *291,* 153–159.
18. Pavelka, M.; Burda, J. V. Theoretical Description of Copper Cu(I)/Cu(II) Complexes in Mixed Ammine-Aqua Environment. DFT and ab Initio Quantum Chemical Study. *Chem. Phys.* **2005,** *312,* 193–204.
19. Stace, A. J.; Shukla, A. K. Preferential Solvation of Hydrogen Ions in Mixed Clusters of Water with Methanol and Ethanol. *J. Am. Chem. Soc.* **1982,** *104,* 5314–5318.
20. Stace, A. J.; Moore, C. Solvation of Hydrogen Ions in Mixed Clusters of Water and Alcohol. *J. Am. Chem. Soc.* **1983,** *105,* 1814–1819.
21. Stace, A. J. Preferential Solvation of Hydrogen Ions in Mixed Water-Amine Ion Clusters. *J. Am. Chem. Soc.* **1984,** *106,* 2306–2314.
22. Walker, N. R.; Wright, R.; Stace, A. J. Stable Gas Phase Complexes of Silver(II). *J. Am. Chem. Soc.* **1999,** *121,* 4837–4844.
23. Cooks, R. G.; Beynon, J. H.; Caprioli, R. M.; Lester, G. R. *Metastable Ions;* Elsevier: Amsterdam, 1973; p. 42.
24. Wu, B.; Duncombe, B. J.; Stace, A. J. Fragmentation Pathways of $[Mg(NH_3)_n]^{2+}$ Complexes: Electron Capture Versus Charge Separation. *J. Phys. Chem. A* **2006,** *110,* 8423–8432.
25. Frisch, M. J.; Trucks, G. W.; Schlegel, H. B.; Scuseria, G. E.; Robb, M. A.; Cheeseman, J. R.; Zakrzewski, V. G.; Montgomery, J. A.; Stratmann, R. E.; Burant, J. C.; Dapprich, S.; Millam, J. M.; Daniels, A. D.; Kudin, K. N.; Strain, M. C.; Farkas, O.; Tomasi, J.; Barone, V.; Cossi, M.; Cammi, R.; Mennucci, B.; Pomelli, C.; Adamo, C.; Clifford, S.; Ochterski, J.; Petersson, G. A.; Ayala, P. Y.; Cui, Q.; Morokuma, K.; Malick, D. K.; Rabuck, A. D.; Raghavachari, K.; Foresman, J. B.; Cioslowski, J.; Ortiz, J. V.; Stefanov, B. B.; Liu, G.; Liashenko, A.; Piskorz, P.; Komaromi, I.; Gomperts, R.; Martin, R. L.; Fox, D. J.; Keith, T.; Al-Laham, M. A.; Peng, C. Y.; Nanayakkara, A.; Gonzalez, C.; Challacombe, M.; Gill, P. M. W.; Johnson, B. G.; Chen, W.; Wong, M. W.; Andres, J. L.; Head-Gordon, M.; Replogle, E. S.; Pople, J. A. *Gaussian 03*; Gaussian, Inc.: Pittsburgh. PA, 1998.
26. Cox, H.; Akibo-Betts, G.; Wright, R. R.; Walker, N. R.; Curtis, S.; Duncombe, B.; Stace, A. J. Solvent Coordination in Gas-Phase $[Mn(H_2O)_n]^{2+}$ and $[Mn(ROH)_n]^{2+}$ complexes: Theory and Experiment. *J. Am. Chem. Soc.* **2003,** *125,* 233–242.
27. Rotzinger, F. P. Performance of Molecular Orbital Methods and Density Functional Theory in the Computation of Geometries and Energies of Metal Aqua Ions. *J. Phys. Chem. B* **2005,** *109,* 1510–1527.
28. Wu, B. Gas-Phase Studies of Multiply Charged Metal-Ligand Complexes, Ph.D. Thesis, The University of Nottingham, 2007.
29. Ishii, K.; Itoh, A.; Okuno, K. Electron-Capture Cross-Sections of Multiply Charged Slow Ions of Carbon, Nitrogen, and Oxygen in He. *Phys. Rev. A* **2004,** *70,* 042716.